β-Cell Neogenesis During Prolonged Hyperglycemia in Rats

Mark Lipsett and Diane T. Finegood

β-cell neogenesis from ductal precursors, and possibly from other pancreatic cell types, contributes to the expansion of β-cell mass during development and after diabetogenic insults in rodents. Using a mathematical model–based analysis of β-cell mass, replication, and size, we recently demonstrated that neogenesis is also quantitatively important to the expansion of β-cell mass during prolonged hyperglycemia. In the present study, we examined the morphological appearance of neogenic focal areas, duct cell replication, and β-cell cluster size distribution in male Sprague Dawley rats infused with either saline or 50% glucose (2 ml/h) for 0, 1, 2, 3, 4, 5, or 6 days. Pancreatic tissue characterized by a high density of small duct-like structures, previously described as neogenic focal areas, were present in glucose-infused rats after 2, 3, or 4 days of infusion. The cross-sectional area of the pancreas characterized as focal tissue peaked after 3 days of infusion at 2.9 ± 0.8%. In contrast to the partial pancreatectomy model of β-cell regeneration, duct cell replication was not increased before or during focal area formation. However, the replication rate of cells in the duct-like structures of the focal areas was twofold greater than in cells of the common pancreatic duct and 15- to 40-fold greater than in cells of small, medium, and large ducts. Duct-cell replication was significantly reduced in small, medium, and large ducts of glucose as compared to saline-infused rats (0.21 ± 0.02 vs. 0.48 ± 0.04%; $P < 0.03$). Duct-associated β-cell mass was not different in glucose- and saline-infused rats ($P = 0.78$), whereas the number of acinar-associated single β-cells increased by 70% after 3 and 4 days of glucose infusion. In addition to small duct-like structures, focal areas had considerable T-cell infiltration (151 ± 30 T-cells/mm^2). There was also an increase in T-cell infiltration in acinar tissue of glucose as compared to saline-infused rats (0.43 ± 0.11 vs. 0.03 ± 0. 01 T-cells/mm^2; $P < 0.0001$). In conclusion, these data suggest that neogenic focal areas in these glucose-infused rats do not arise from replication and differentiation of ductal progenitor cells. Rather, acinar cell transdifferentiation into β-cells and acinar cell dedifferentiation into neogenic focal areas lead to new β-cell formation during prolonged hyperglycemia. *Diabetes* 51:1834–1841, 2002

From the Diabetes Research Laboratory, School of Kinesiology, Simon Fraser University, Burnaby, British Columbia, Canada.

Address correspondence and reprint requests to Diane T. Finegood, PhD, Diabetes Research Laboratory, School of Kinesiology, Simon Fraser University, 8888 University Dr., Burnaby, British Columbia, Canada V5A 1S6. E-mail: finegood@sfu.ca.

Received for publication 5 September 2000 and accepted in revised form 16 January 2002.

BrdU, 5-bromo-2′deoxyuridine; IFN-γ, γ-interferon; PDX-1, pancreatic duodenal homeobox 1.

Over the past few decades, we have come to appreciate that the β-cell mass is dynamic, with a significant capacity for adaptation to changes in insulin demand (1). Increases in β-cell mass may occur through increased β-cell replication, increased β-cell size, decreased β-cell death, and differentiation of β-cell progenitors (neogenesis) (2). Neogenesis is an important component of β-cell mass expansion during development, and also has been shown to contribute to increases in β-cell mass in juvenile and adult rodent models (2–4). After 90% partial pancreatectomy in rats age 5–6 weeks, focal areas consisting of small duct-like structures appear to give rise to new endocrine and exocrine pancreatic tissue (5). In this model, duct cell replication rates are elevated before and during focal area formation, suggesting that the duct-like structures in the focal areas arise through the proliferation of existing ducts (5). The replication rate of the cells making up the duct-like structures is also high, but the focal areas disappear by 10 days after the pancreatectomy, suggesting that the focal areas give rise to new endocrine and exocrine tissue. This is consistent with the observation that replication generally occurs before cellular differentiation (6). These data suggest that expansion of the β-cell mass by replication and then differentiation of duct cell progenitors is an important pathway of β-cell neogenesis.

Focal areas with duct-like structures have also been observed in other models of β-cell regeneration, including pancreatic duct ligation (7) and transgenic mice overexpressing γ-interferon (IFN-γ) on the human insulin promoter (8). Complete ligation of the pancreatic duct leads to an inflammatory response, atrophy of the distal portion of the pancreas, and loss of normal acinar cells, followed by their replacement with highly replicating duct-like structures. Subsequently, there is an increase in β-cell mass in the form of small islets, β-cell clusters, and single β-cells (7). In the transgenic mouse model, focal areas with small duct-like structures form after an immune response stimulated by the overexpression of IFN-γ in β-cells (8). New β-cells form through differentiation of the duct-like structures after destruction of the original islets. The mechanism underlying focal area formation in these models is unclear, but cytokines released from infiltrating leukocytes are thought to play a role (9,10). Other mechanisms may also be important for focal area formation, given that no inflammation has been noted in focal areas after partial pancreatectomy (5).

Additional pathways for β-cell neogenesis may also be important to β-cell regeneration. Direct duct–to–β-cell

transdifferentiation and transdifferentiation from other progenitors has been demonstrated in these and other models (3,11,12). Direct duct-to-β-cell transdifferentiation is suggested by observations of insulin-positive duct cells and islets budding from ducts in developing rodent pancreas, and in many models of β-cell regeneration, including partial duct obstruction, duct ligation, and during chronic glucose infusion (3,10,13). Transdifferentiation from other endocrine cell types to β-cells is suggested by the time-dependent appearance of double positive (somatostatin/pancreatic duodenal homeobox-1 [PDX-1]) cells followed by triple positive (somatostatin/PDX-1/insulin) cells in the islets of mice treated with a high dose of streptozotocin (11). Coexpression of exocrine and endocrine markers and in vitro differentiation of rat acinar tumor cells suggests that exocrine tissue may also be a source of new β-cells (12,14).

We recently demonstrated that β-cell neogenesis is also an important component of β-cell mass dynamics during prolonged hyperglycemia (15). We have found that β-cell neogenesis contributes to the expansion of the β-cell mass after several days of glucose infusion. Our mathematical model–based approach, along with a detailed assessment of β-cell mass, replication rate, and size, allowed us to deduce the contribution of β-cell neogenesis to β-cell mass dynamics during chronic glucose infusion. This inferential method does not provide any information regarding the mechanism underlying the β-cell neogenesis. However, we reported for the first time the appearance of focal areas in glucose-infused animals (15), which led to the hypothesis on which this study was based—that is, that neogenesis occurred by replication of ductal progenitors and then differentiation into β-cells. Here we report on a detailed quantitative morphometric assessment of β-cell neogenesis in the same group of rats infused with glucose (2 ml/h of 50% glucose) or saline for 0, 1, 2, 3, 4, 5, or 6 days. We determined the frequency and size of focal areas; duct cell replication rates in small, medium, large, common, and focal area duct cells; and β-cell cluster size, distribution, and association with ducts, exocrine, and focal area tissue. Lymphocytic infiltration into acinar and focal area tissue was also quantified. Our results demonstrated that β-cell neogenesis is an important component of β-cell mass expansion during prolonged hyperglycemia. In contrast to our expectation, however, focal areas did not appear to arise from ductal progenitor cells. Rather, acinar cell dedifferentiation may make a significant contribution to β-cell mass expansion in this model.

RESEARCH DESIGN AND METHODS

Animals. In the present study, tissue samples from our previous study were used (15). In brief, adult male Sprague Dawley rats were chronically catheterized (jugular vein) and infused with saline or glucose. After a 3- to 5-day recovery period, rats were infused with either 0.45% saline ($n = 45$) or 50% glucose in 0.45% saline ($n = 60$) at 2 ml/h for 0, 1, 2, 3, 4, 5, or 6 days. Then 6 h before being killed, rats were injected intraperitoneally with 100 mg/kg 5-bromo-2′deoxyuridine (BrdU; Amershan Canada, Oakville, ON, Canada). At termination, rats were anesthetized with sodium-pentobarbitol (35 mg/kg body wt, i.p.) and a cardiac puncture was performed. The pancreas was removed and the rat was killed by a diaphragm incision. The pancreas was blotted and cut into three pieces (duodenal, middle, and splenic), weighed, fixed in Bouin's solution overnight, washed in cold water, and stored in 10% formalin until embedding in paraffin wax. All procedures involving animals were performed in accordance with the Guidelines of the Canadian Council on Animal Care.

Immunohistochemistry. Sections 4- to 5-μm thick were taken from each of the three pieces of pancreas and de-waxed in xylene. Endogenous peroxidase activity was blocked with a 0.3% solution of hydrogen peroxide. The sections were then washed with PBS and incubated with 10% lamb serum in PBS for 30 min at room temperature. Slides were stained with one or more primary antibodies, including insulin (guinea pig anti-porcine, 1:2000; Dako Diagnostics Canada, Mississauga, Canada); a cocktail of antibodies to glucagon, somatostatin, and pancreatic polypeptide (rabbit anti-human, 1:2000; Dako); BrdU (mouse monoclonal anti-BrdU, 1:100, Amersham Canada); and CD3 (rabbit anti-human, 1:1500, Dako). Slides stained for CD3 were incubated with citrate buffer for 30 min at 90°C for antigen retrieval before primary antibody application. Slides were incubated with primary antibodies overnight at 4°C before being washed in PBS and incubated with the secondary antibodies for 1 h at room temperature (1:500; biotinylated goat anti-guinea pig IgG, biotinylated goat anti-mouse IgG, or biotinylated goat anti-rabbit IgG; Dako). Sections were then washed in PBS, incubated with avidin-biotin complexed with horseradish peroxidase (1:1000; Vectastain Elite ABC Kit, Vector Laboratories Canada, Burlington, Canada) for 1 h, and then developed using 3,3′-diaminobenzidine tetrahydrochoride (Sigma-Aldrich Canada, Oakville, Canada). All slides were counterstained with Harris' hematoxylin (Sigma-Aldrich).

Focal area analysis. Focal areas were defined as areas of tissue consisting of small duct-like structures with an apparent infiltration of leukocytes (Fig. 1*A*). These areas were clearly delineated, with defined borders usually juxtaposed to normal acinar tissue. One slide from each of the three parts of each pancreas (stained with a cocktail of antibodies to glucagon, somatostatin, and pancreatic polypeptide) were relabeled and randomized so as to blind the viewer to the treatment group. Each slide was examined using a light microscope (Olympus Model BX40; Carsen Group) at ×200 for the presence or absence of focal area tissue. To determine the cross-sectional area of focal tissue, sections were systematically sampled using an image analysis system (Northern Eclipse; Empix Imaging, Mississauga, Canada). Slides were examined in 1.0 × 1.5-mm increments, resulting in the assessment of 70 ± 5 fields/slide and 82 ± 5% of the total pancreatic section. Focal tissue area was quantified by capturing each field and hand tracing focal areas within the captured images. The thresholding option was used to quantify the cross-sectional areas occupied by tissue and to subtract unstained areas (white space) not occupied by any tissue. Focal area sizes are reported as the cross-sectional area of focal tissue as a percent of total pancreatic tissue area.

Duct size and replication rate. To determine the replication rate of duct cells from small, medium, large, common, and focal area ducts, sections stained with cocktail, anti-BrdU antibodies were scanned, and all duct cells were counted. BrdU incorporation was assessed for rats infused with either glucose ($n = 26$) or saline ($n = 24$) for 0–4 days. One slide from each of the three portions of the pancreas was assessed, and an average of 17,541 ± 522 duct cells/animal were counted. Duct size category was assigned based on a qualitative assessment of the number of nuclei in the duct circumference, the amount of encapsulating connective tissue, the sectioning angle of the duct, and the general morphological appearance of the duct, similar to the procedure used by Githens et al. (16). Duct cell replication rates for each duct size were determined as the percentage of nuclei stained positive for BrdU for each animal.

β-cell cluster size distribution. β-cell cluster size distribution was determined from three slides (one duodenal, one middle, and one splenic) for each rat. Slides stained with anti-insulin antibody were randomized, relabeled, and analyzed using a light microscope (Olympus; final magnification ×350) and image analysis software. All insulin-positive β-cell clusters of one or more cells were loosely traced and the size of the cluster within the trace was determined by using the thresholding option. We have used the term "β-cell cluster" rather than "islet" because clusters were identified on the basis of insulin antibody staining and did not include identification of other endocrine and nonendocrine cell types found in islets. The association of each insulin-positive cluster with acinar, duct, or focal area tissue was made according to the type of tissue bordering at least 50% of the cluster. The incidence of β-cell clusters is reported as the average across animals in a treatment group of the sum from three slides examined per animal of β-cell clusters detected for each tissue association (acinar, duct, or focal area) and size (single, small, medium, or large) category.

To establish category size cutoffs, the size of a single β-cell was determined by measuring the cross-sectional area of insulin-positive clusters with only one nuclei (Fig. 1*B*). Single β-cell size was determined for both acinar and duct-associated ($n = 5$ each) single β-cells from saline- and glucose-infused rats ($n = 13$; one from each day and type of infusion). Acinar-associated single β-cells were significantly larger than duct-associated single β-cells (152 ± 8 vs. 114 ± 7 μm^2; $P < 0.001$). All β-cell clusters with areas less than or equal to the average single β-cell size (≤152 μm^2 for acinar, ≤114 μm^2 for duct) were

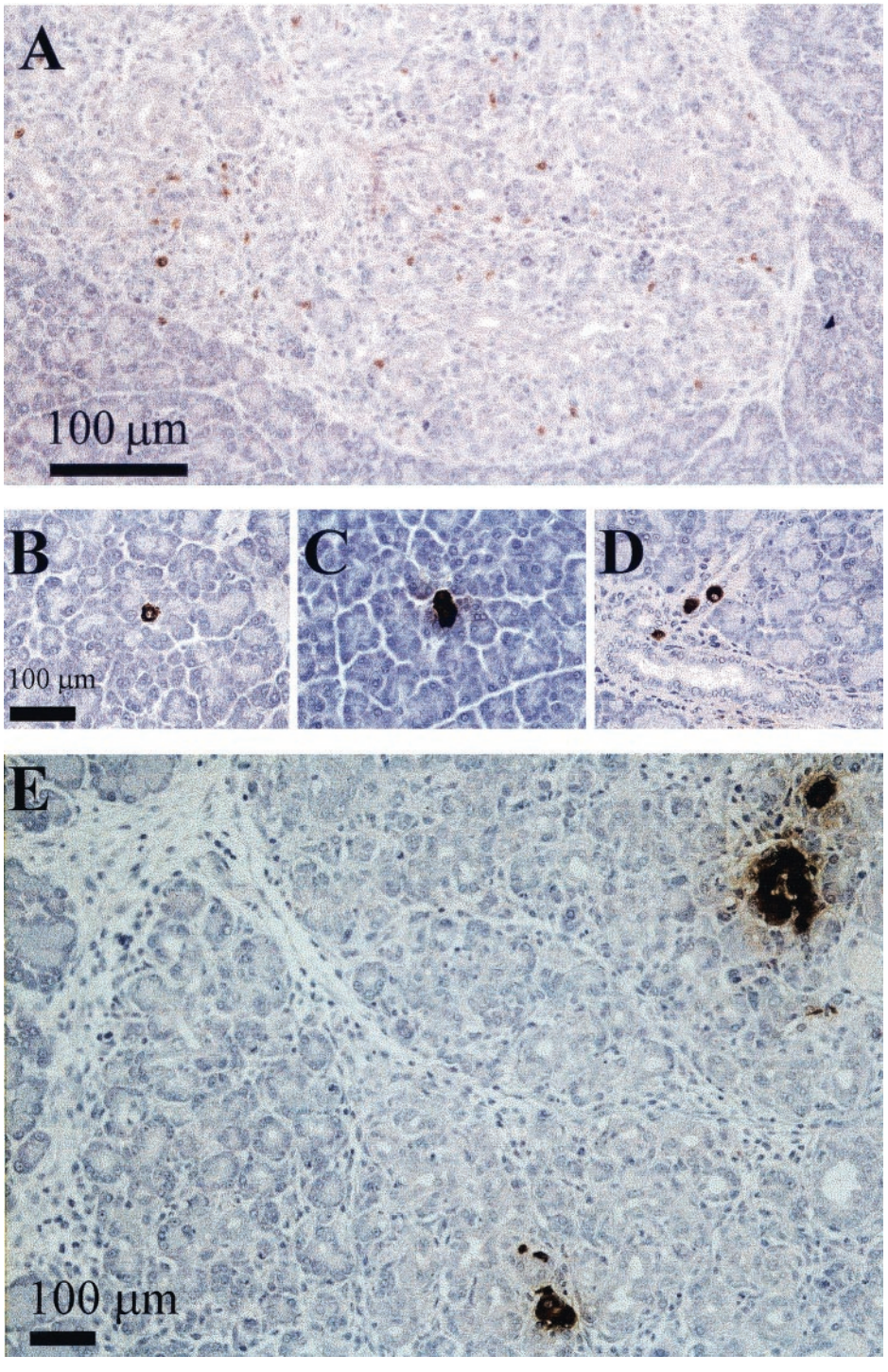

FIG. 1. *A*: Focal area from a 3-day glucose-infused rat with infiltrating T-cells (brown membrane staining). *B*: An acinar-associated single β-cell. *C*: A small acinar-associated β-cell cluster. *D*: Duct-associated single β-cell clusters from a 4-day saline-infused rat. *E*: Focal area–associated β-cells from a 3-day glucose-infused rat.

categorized as single β-cells (Fig. 1*B*). All β-cell clusters with areas greater than the average single β-cell size and less than or equal to three times the average single β-cell size were considered small extra-islet β-cell clusters (Fig. 1*C*). The remaining insulin-positive β-cell clusters were arbitrarily divided into medium and large clusters of 15,000 μm^2.

T-cell infiltration. The number of T-cells/mm^2 was determined for acinar and focal tissue in rats infused for 0, 1, 2, 3, or 4 days from slides stained with anti-CD3 antibodies. The number of $CD3^+$ T-cells associated with acinar tissue were counted using a light microscope (Olympus; ×400). A T-cell was considered to be acinar associated when it was bound on all sides by acinar tissue. Intravascular T-cells were not counted. The total number of acinar-associated T-cells per animal was divided by the total area of acinar tissue determined from previous β-cell mass measurements to obtain a T-cell infiltration index for each animal. The density of T-cells in focal areas was determined using an image analysis system to measure focal tissue area and count the number of $CD3^+$ T-cells in the focal areas. The T-cell density is reported as the total number of focal area T-cells divided by the total focal tissue area for each rat.

Statistical analysis. Statistical analyses were performed using SAS System for Windows (Release 6.12; SAS Institute, Cary, NC) and SYSTAT for Windows (Version 6.0; SYSTAT, Evanston, IL). One, two, or three-way ANOVA or the Wilcoxon nonparametric analysis was performed where appropriate using the following factors: infusion type (glucose and saline), day of infusion (0–6), duct size (small, medium, large, common, and focal), or β-cell cluster size (single, small, medium, and large). Five animals were used for each comparison unless otherwise reported. Because there was only one group of animals for day 0, the data from these animals were considered as day 0 for both saline and glucose time-dependent comparisons. Post hoc individual comparisons were conducted when deemed appropriate by an omnibus ANOVA measurement. Differences were con-

TABLE 1
Number of rats with focal areas present in the pancreas

Day of infusion	Saline		Glucose		
	n	n with focal areas	n	n with focal areas	%
0	10	0	10	0	0
1	7	0	10	0	0
2	5	0	10	3	30
3	8	0	16	9	56
4	6	0	13	2	15
5	5	0	7	0	0
6	4	0	4	0	0

sidered to be significant at $P < 0.05$. All results are expressed as means ± SE.

RESULTS

Focal areas. Pancreatic focal areas (Fig. 1*A*) were present in rats infused with glucose for 2, 3, or 4 days but not in any saline-infused rats (Table 1). Focal areas varied in size from 0.1 to 14.9% of the total pancreas area (Fig. 2). Focal areas were most apparent after 3 days of glucose infusion, averaging 2.9 ± 0.8% of the pancreatic tissue.

Duct cell replication rates. The replication rate of duct cells from small, medium, large, or common ducts was not elevated before or during the appearance of focal areas (Fig. 3). By three-way ANOVA, there was a significant effect of duct size ($P < 0.0001$) and length of infusion ($P = 0.048$), but not of treatment ($P = 0.075$), on duct cell replication rate. The replication rate was 7- to 20-fold greater in common duct cells than in small, medium, and large duct cells, whereas the replication rate of focal area duct cells was 2-fold greater than in the common duct (Fig. 4). Although treatment was not a significant effect by three-way ANOVA, the replication rate of small ($P = 0.0016$), medium ($P < 0.0001$), and large ($P = 0.009$) duct cells was significantly greater in saline- than in glucose-infused animals by one-way ANOVA (Fig. 4). The effect of length of infusion observed by three-way ANOVA was attributable to suppression of BrdU incorporation by glucose over time in medium ($P = 0.0068$) and large ($P = 0.0272$) ducts (Fig. 3), and was not attributable to any time-dependent effects in small or common ducts or in saline-infused animals.

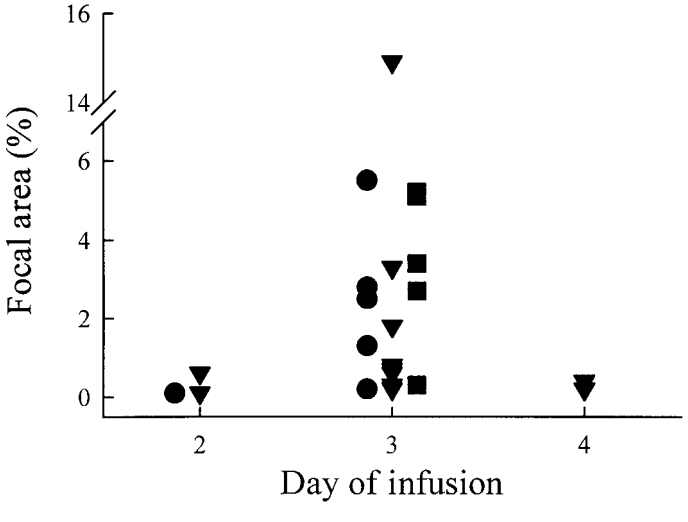

FIG. 2. Percent of each tissue section occupied by focal areas in glucose-infused rats. In some animals, focal areas were detected in more than one of the three samples from a given animal, making the total number of sections with focal areas greater than the number of animals having focal areas, as indicated in Table 1. ●, duodenal portion; ▼, middle portion; ■, splenic portion.

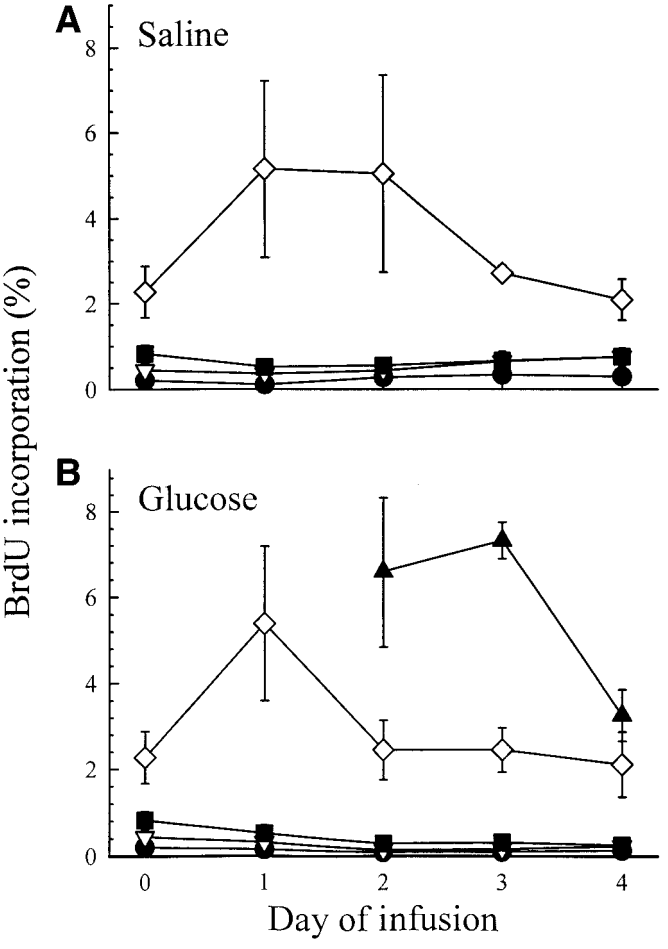

FIG. 3. Duct cell replication rates from rats infused with saline (*A*) and glucose (*B*) for 0–4 days. ●, small ducts; ▽, medium ducts; ■, large ducts; ◇, common ducts; ▲, focal area ducts. $n = 5$ for all glucose- and saline-infused rats for each day of infusion except for the following: $n = 6$ for days 2 and 4 of glucose infusion, $n = 10$ for day 3 of glucose infusion, $n = 4$ for day 2 of saline infusion. Statistical differences determined by three-way ANOVA are reported in the text.

β-cell mass. Total β-cell mass determined by insulin antibody staining (Fig. 5) increased progressively in glucose-infused animals to an approximately twofold increase over saline-infused animals by 6 days of infusion (similar to results obtained using the cocktail of antibodies to glucagon, somatostatin, and pancreatic polypeptide [15]).

Duct-associated β-cell mass constituted ~1% of the total β-cell mass (Fig. 1*D*). There was no difference, however, in the mass of β-cells associated with ducts during glucose and saline infusion ($P = 0.78$) (Table 2). The mass of β-cells found in focal areas (0.049 ± 0.021 mg) was similar to the mass of β-cells associated with ducts (0.055 ± 0.005 mg). The remaining 98–99% of the β-cell mass was associated with acinar tissue. The mass of acinar-associated single β-cells increased 63% in glucose- versus saline-infused animals after 4 days of infusion (0.052 ± 0.007 vs. 0.032 ± 0.003 mg, respectively) to account for <1% of the total β-cell mass (Table 3).

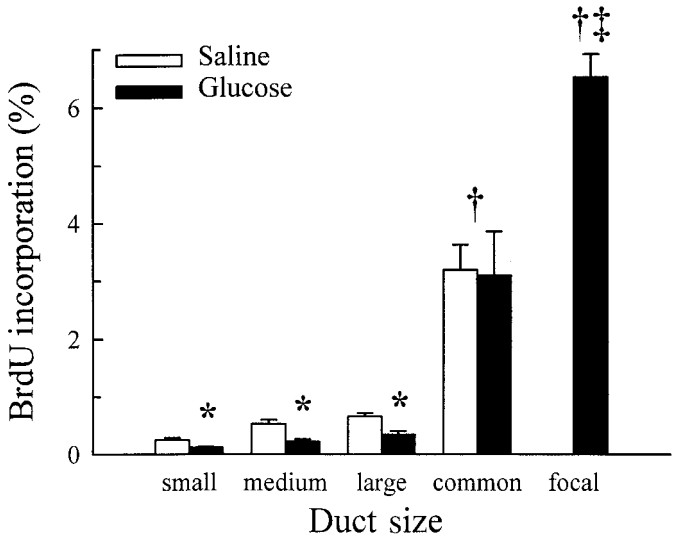

FIG. 4. Average duct cell replication rates. *$P < 0.05$ saline vs. glucose; †$P < 0.001$ vs. small, medium, and large ducts; ‡$P < 0.05$ vs. common ducts.

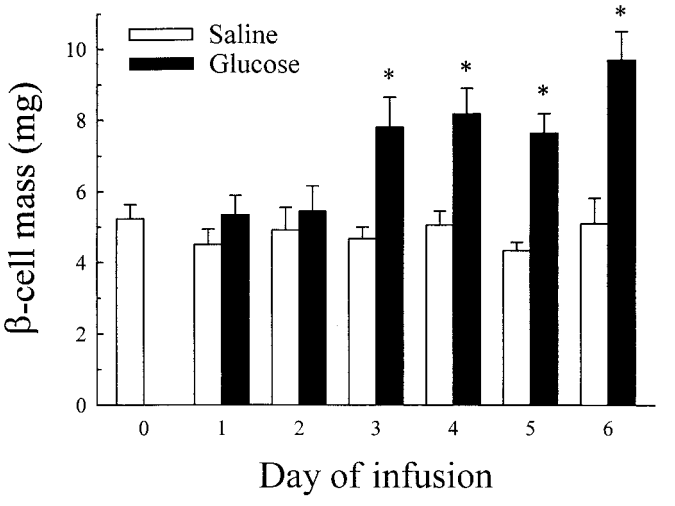

FIG. 5. Average β-cell mass as determined by insulin antibody staining and image analysis. $n = 5$ for all each treatment for each day of infusion except for $n = 6$ for day 4 of glucose infusion and $n = 4$ for day 6 of glucose and saline infusion.

β-cell size distribution. As with total duct-associated β-cell mass, there was no effect for type of infusion (glucose or saline, respectively) on the number of single (27.0 ± 2.7 vs. 26.4 ± 1.8), small (16.9 ± 1.6 vs. 17.8 ± 1.1), or medium (6.7 ± 0.8 vs. 6.5 ± 0.7) β-cell clusters associated with ducts ($P = 0.97$). Likewise, there was no effect of infusion type on the average size of single, small, or medium duct-associated β-cell clusters ($P > 0.35$) (Table 2).

There were focal area−associated insulin-positive clusters found in all animals with focal areas investigated for β-cell mass (day 2: $n = 1$, day 3: $n = 4$). The total number of β-cell clusters associated with focal areas ranged was 2–35 per animal. In all, 58% of insulin-positive clusters in focal areas were <152 μm^2 in cross-sectional area. There was also an increase in the incidence of acinar-associated single β-cells during glucose infusion as compared to saline infusion. The number of acinar-associated single β-cells was increased by 70% at 3 and 4 days of glucose infusion (Fig. 6*A*). The increased number was associated with a decrease in the average single β-cell size (Fig. 6*B*). As expected, when viewing total β-cell mass dynamics (Fig. 5), there was a significant effect of infusion type on the number of medium ($P = 0.043$) and large acinar-associated β-cell clusters ($P < 0.0001$). For large β-cell clusters, there was a significant increase in both number and average cluster size with days of glucose infusion, so that by 6 days of glucose infusion, the frequency had increased twofold and the average cluster size had increased by 30% in glucose- compared to saline-infused animals.

T-cell infiltration. Acinar T-cell infiltration was elevated by ~10-fold in glucose- as compared to saline-infused rats ($P < 0.001$, Fig. 7). There was an effect of day of infusion on T-cell infiltration in glucose-infused rats ($P = 0.0442$), peaking at 0.74 ± 0.27 T-cells/mm^2 after 2 days of infusion. Along with a diffuse T-cell infiltration into the acinar tissue of glucose-infused rats, there were distinct areas with a high density of T-cells. Focal areas in glucose-infused rats had a very high density of T-cells, ~350 times greater than in acinar tissue (151 ± 30 T-cells/mm^2) (Fig. 1).

DISCUSSION

β-cell neogenesis is known to be important during development and to contribute to β-cell regeneration after diabetogenic insults, such as 90% partial pancreatectomy and after administration of a high dosage of streptozotocin (5,11). The present study provided the first quantitative morphometric evidence that β-cell neogenesis also occurs during prolonged hyperglycemia. These data support our

TABLE 2
Duct-associated β-cell mass and duct-associated average cluster size

	β-cell mass (mg)		Single β-cells size (μm^2)		Small β-cell cluster size (μm^2)		Medium β-cell cluster size (μm^2)	
Day	Saline	Glucose	Saline	Glucose	Saline	Glucose	Saline	Glucose
0	0.048 ± 0.005	—	63.6 ± 3.0	—	185.4 ± 2.3	—	763 ± 119	—
1	0.068 ± 0.014	0.039 ± 0.008	58.6 ± 4.1	62.2 ± 1.6	186.0 ± 2.3	193.2 ± 3.6	1318 ± 275	1083 ± 325
2	0.041 ± 0.007	0.052 ± 0.019	60.8 ± 1.5	60.6 ± 4.3	185.2 ± 6.6	185.2 ± 9.0	978 ± 316	1195 ± 349
3	0.057 ± 0.022	0.063 ± 0.013	65.0 ± 3.1	54.4 ± 4.6	186.0 ± 6.2	180.0 ± 8.6	980 ± 328	1430 ± 243
4	0.043 ± 0.020	0.074 ± 0.020	62.0 ± 3.2	64.3 ± 2.6	171.4 ± 7.2	189.3 ± 6.8	948 ± 309	1326 ± 242
5	0.030 ± 0.006	0.058 ± 0.028	66.6 ± 4.8	61.6 ± 2.9	185.2 ± 6.9	179.8 ± 11.9	654 ± 104	1514 ± 614
6	0.066 ± 0.023	0.073 ± 0.014	64.3 ± 1.6	61.3 ± 1.5	183.5 ± 4.4	189.3 ± 8.3	1031 ± 278	954 ± 113

Data are means ± SE.

TABLE 3
Acinar-associated β-cell mass dynamics according to size of cluster

	Single β-cells (≤152 μm²)		Small islet clusters (153–456 μm²)		Medium islet clusters (457–15,000 μm²)		Large islet clusters (>15,000 μm²)	
Day	Saline	Glucose	Saline	Glucose	Saline	Glucose	Saline	Glucose
0	0.031 ± 0.002	—	0.175 ± 0.007	—	2.79 ± 0.19	—	2.19 ± 0.32	—
1	0.043 ± 0.002	0.035 ± 0.004	0.175 ± 0.009	0.153 ± 0.010	2.57 ± 0.11	2.64 ± 0.23	1.65 ± 0.40	2.48 ± 0.38
2	0.030 ± 0.003	0.035 ± 0.002	0.143 ± 0.012	0.159 ± 0.009	2.65 ± 0.25	2.61 ± 0.18	2.04 ± 0.43	2.59 ± 0.56
3	0.039 ± 0.003	0.043 ± 0.007	0.177 ± 0.018	0.158 ± 0.013	2.64 ± 0.13	3.02 ± 0.27	1.76 ± 0.23	4.47 ± 0.60*
4	0.032 ± 0.004	0.052 ± 0.007*	0.156 ± 0.010	0.190 ± 0.018	2.59 ± 0.19	3.24 ± 0.31	2.23 ± 0.20	4.61 ± 0.47*
5	0.036 ± 0.006	0.044 ± 0.002	0.145 ± 0.013	0.153 ± 0.011	2.61 ± 0.09	2.77 ± 0.16	1.52 ± 0.26	4.61 ± 0.57*
6	0.036 ± 0.006	0.044 ± 0.005	0.178 ± 0.004	0.168 ± 0.005	2.71 ± 0.22	3.61 ± 0.21*	2.11 ± 0.59	5.78 ± 0.86*

Data are means ± SE. *$P < 0.05$ vs. saline.

previous model-based conclusion that β-cell neogenesis contributes to β-cell mass expansion during chronic glucose infusion (15). The quantitative histological analyses performed in the present study suggest that neogenic β-cells may arise through differentiation of acinar tissue into focal areas and insulin-positive β-cells.

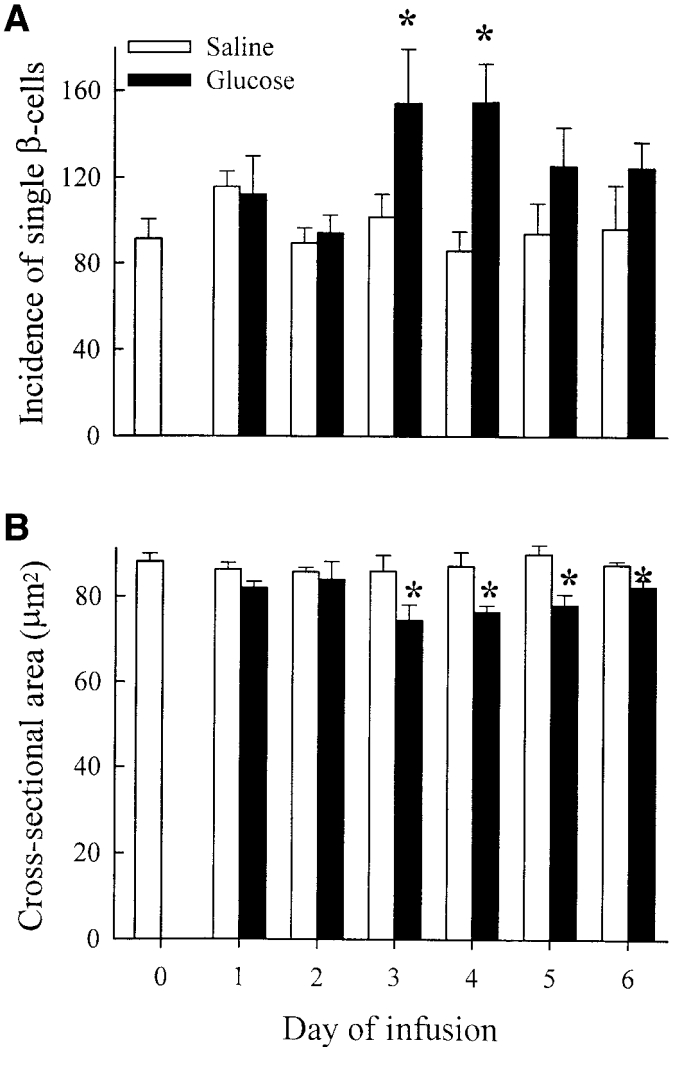

FIG. 6. Frequency of acinar-associated single β-cells (*A*) and average size of acinar-associated single β-cells (*B*) in glucose- and saline-infused rats. $n = 5$ for all each treatment for each day of infusion except as indicated in legend for $n = 6$ for day 4 of glucose infusion and $n = 4$ for day 6 of glucose and saline infusion *$P < 0.05$ vs. day 0.

Focal areas. Areas of pancreatic tissue with many small duct-like structures have been called focal areas (5). These focal areas are thought to give rise to new endocrine and exocrine tissue, deduced in part from their transient appearance after diabetogenic insults (e.g., partial pancreatectomy) and before or in association with increases in β-cell mass (5,7,8). Focal areas appeared transiently in our glucose-infused rats, but were not apparent in the saline-infused animals (Fig. 1 and Table 1). Focal areas have not been previously described in glucose-infused rats, possibly because their peak appearance occurred after 3 days of glucose infusion (Table 1 and Fig. 2). In previous reports, pancreas morphology was examined after 1, 2, or 4 days of chronic glucose infusion (13,17). Although small focal areas (constituting <1% of the pancreas area) were observed in 5 of 23 animals studied after 2 or 4 days of glucose infusion, the majority of rats (56%) infused with glucose for 3 days had focal areas that constituted up to 15% of the total pancreas area (Table 1, Fig. 2).

After partial pancreatectomy, the cells of the duct-like structures in focal areas replicate at a high rate (5). Likewise, the duct-like structures thought to give rise to new β-cells after duct ligation or overexpression of IFN-γ in the β-cell are highly proliferative (7,8). Similarly, the cells of the duct-like structures in the focal areas found in our glucose-infused animals replicated at a rate that was

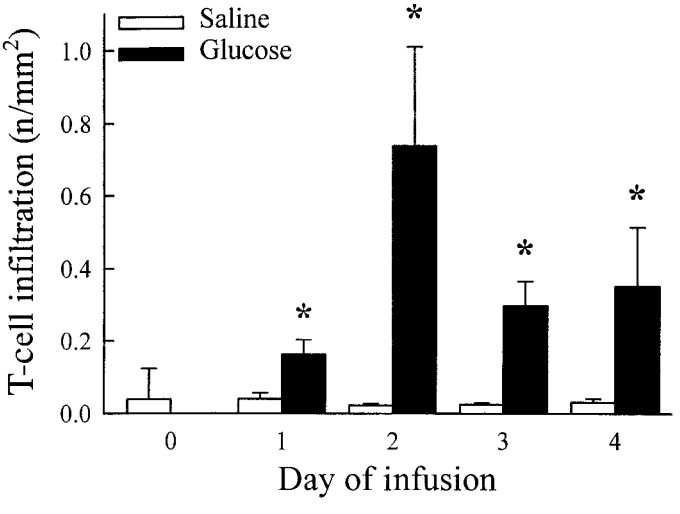

FIG. 7. Acinar T-cell infiltration indexes of both saline- and glucose-infused rats. $n = 5$ for all glucose- and saline-infused rats for each day of infusion except for $n = 8$ for day 2 of glucose infusion and $n = 6$ for day 4 of glucose infusion. *$P < 0.05$ vs. saline.

2-fold greater than for cells in the common duct and 15- to 40-fold greater than in cells lining the small, medium, and large ducts (Fig. 4). The high proliferative rate of these duct-like structures along with the disappearance of the focal areas suggests that the majority of the new cells differentiate into endocrine or exocrine cell types. Thus the focal areas observed in our glucose-infused rats likely contribute to an increase in β-cell neogenesis.

Single β-cells. Single β-cells surrounded by acinar, focal, or even ductal tissue are thought to arise primarily through differentiation from the surrounding cell type (7,18), although some cells may arrive at a given location after migration from their tissue origin (19). It is also possible that single cells are derived from another cell type not visible in the plane of the section, but the appearance of single cells and small β-cell clusters has been used as an index of new β-cell formation (7,18,20). In the present study we found a high incidence of single β-cells in focal areas and in acinar tissue after 3 and 4 days of glucose infusion (Fig. 6). In support of the idea that these single β-cells represent newly formed β-cells is the finding that the average acinar-associated single β-cell size decreased concomitantly with the increased number of cells. Scaglia et al. (21) have suggested that a decrease in cell size might be indicative of newly differentiated β-cells. Whether these single β-cells arise from differentiation of duct-like cells in focal areas or from transdifferentiation of exocrine cells could not be determined from the present study. These data clearly indicate that there is an increase in the number of newly formed β-cells from these two sources after 3 days of glucose infusion leading to an increased potential for β-cell mass expansion.

In contrast to the high frequency of single β-cells in focal areas and the increased frequency of single β-cells in acinar tissue after 3 days of glucose infusion, there was no increase in the frequency of duct-associated single β-cells in glucose-infused rats. Single β-cells in ducts likely arise from replication and then differentiation of a ductal progenitor. Presumably, these cells then either replicate to form small duct-associated β-cell clusters or migrate into the surrounding tissue (19,22). Cells migrating into exocrine tissue probably develop into small β-cell clusters and new islets. Alternatively, these cells may migrate to become part of established islets (23). Thus it is possible that the rate of new β-cell formation from ductal progenitors could increase without an increase in the number of duct-associated β-cells (i.e., if migration into the surrounding tissue increases at the same rate as replication and differentiation of the duct cells). However, the suppression of duct cell replication rates by glucose (Fig. 4) and the lack of an effect of glucose on the frequency, average size, or mass of duct-associated β-cell clusters (Table 2) suggests that direct duct-to-β-cell transdifferentiation does not contribute to the increase in β-cell neogenesis in our glucose-infused rats. Although local areas of increased duct proliferation may have been missed by our sampling method, on average, duct proliferation was reduced in glucose infused rats, suggesting that this is not a quantitatively important pathway for β-cell neogenesis during glucose infusion.

These results are in direct contrast to the recent report by Bernard et al. (13). After 24 h of clamping plasma glucose at ~22 mmol/l, they observed a high rate of BrdU incorporation into duct cells and a large number of endocrine cells within or budding from ducts in glucose- as compared to saline-infused rats (13). Whether the differences between the study of Bernard et al. (13) and the present data are attributable to differences in rat strain, the plasma glucose level achieved after 24 h (~35 mmol/l in the present study), those investigators' qualitative judgement versus our quantitative assessment, or some other explanation, requires clarification. That the differences in neogenic indexes are a result of differences in experimental conditions (rat strain or glucose level), however, is suggested by the finding of Bernard et al. of a 50% increase in total β-cell mass after 24 h and our finding of no increase in β-cell mass after the same length of infusion (13).

Origin of focal areas. Our quantitative analysis of duct cell replication rates led us to reject our original hypothesis that the focal areas arise from ductal progenitor cells. Bonner-Weir et al. (5) demonstrated sequential waves of duct cell proliferation beginning in the common duct and progressing from large through small ducts before focal area formation in partially pancreatectomized rats. In the present study, there was no increase in duct cell proliferation before or during the time of focal area formation in glucose-infused rats (Fig. 3). In fact, glucose infusion led to a significant decrease in the proliferation rate of cells in small, medium, and large ducts (Fig. 4). Because increased proliferation of ductal progenitors likely precedes the formation of focal areas from ducts, these data suggest that the focal areas in our glucose-infused rats were not of ductal origin.

If the focal areas do not arise from the proliferation of ducts, could they arise through dedifferentiation of acinar tissue? Wang et al. (7) have suggested that acinar cell dedifferentiation is the source of focal areas in the duct ligation model of β-cell mass expansion. In this model, immune cell infiltration of the acinar tissue and upregulation of growth factors and cytokines is thought to stimulate the differentiation of acinar tissue into focal area tissue (10). In the present study, acinar T-cell infiltration was elevated in glucose-infused rats before and during focal area formation. In addition, the density of acinar T-cell infiltration was highly variable after 2 days of glucose infusion, suggesting that immune cell infiltration immediately preceded focal area formation. The T-cell infiltration index of focal areas in the glucose-infused rats was similar to that found in human pancreatitis (24). Pancreatitis is thought to result from intraductal precipitation of proteins leading to duct obstruction (25). Hyperosmotic glycemic infusions lead to decreased fluid content in the pancreas (26) and as a result may lead to duct protein precipitation and a form of duct obstruction in glucose-infused rats. Taken together, these data are also consistent with the idea that the focal areas observed in our glucose-infused rats arise through dedifferentiation of acinar tissue, rather than from proliferation of ductal precursors. To determine whether this dedifferentiation and probable redifferentiation into both endocrine and exocrine tissue is attributable to ductal obstruction caused by the infusion of the hyperosmolar glucose solution

requires additional control studies with a hyperosmolar solution at normal glucose levels.

Summary. Through a detailed time-dependent morphometric analysis of pancreases from rats infused with glucose for 0, 1, 2, 3, 4, 5, and 6 days, we have been able to demonstrate that β-cell neogenesis contributes to a glucose-induced expansion of the β-cell mass. The decrease in duct cell replication and the absence of an increase in duct-associated β-cell frequency or mass all suggest that the increase in β-cell neogenesis is not from duct-associated stem cells. The increase in acinar-associated single β-cells, the time-dependent leukocyte infiltration of the acinar tissue before focal area formation, and the high frequency of focal area−associated single β-cells all suggest that acinar tissue, through both direct (acinar to β-cell) and indirect (acinar to focal area to β-cell) pathways may be responsible for the increased β-cell neogenesis during prolonged hyperglycemia.

ACKNOWLEDGMENTS

These studies were supported by a grant from the Medical Research Council (MT10574) of Canada.

We are grateful for the technical assistance of Warren E. Fieldus in producing the image analysis algorithms and Mauro Castellarin for his assistance with morphometric assessments. Many people contributed to the experiments that provided the samples analyzed in the present report, including M. Dawn McArthur, Dan Tzur, Abha Dunichand-Hoedl, Narinder Dhatt, Jamie T. Lewis, Gerald LaChance, and Dr. Jan Przysiezniak.

REFERENCES

1. Bonner-Weir S: Perspective: postnatal pancreatic beta cell growth. *Endocrinology* 141:1926–1929, 2000
2. Finegood DT, Scaglia L, Bonner-Weir S: Dynamics of beta-cell mass in the growing rat pancreas: estimation with a simple mathematical model. *Diabetes* 44:249–256, 1995
3. Rosenberg L: In vivo cell transformation: neogenesis of beta cells from pancreatic ductal cells. *Cell Transplant* 4:371–383, 1995
4. Bouwens L, Kloppel G: Islet cell neogenesis in the pancreas. *Virchows Arch* 427:553–560, 1996
5. Bonner-Weir S, Baxter LA, Schuppin GT, Smith FE: A second pathway for regeneration of adult exocrine and endocrine pancreas: a possible recapitulation of embryonic development. *Diabetes* 42:1715–1720, 1993
6. Beresford WA: Direct transdifferentiation: can cells change their phenotype without dividing? *Cell Differ Dev* 29:81–93, 1990
7. Wang RN, Kloppel G, Bouwens L: Duct- to islet-cell differentiation and islet growth in the pancreas of duct-ligated adult rats. *Diabetologia* 38:1405–1411, 1995
8. Gu D, Lee MS, Krahl T, Sarvetnick N: Transitional cells in the regenerating pancreas. *Development* 120:1873–1881, 1994
9. Arnush M, Gu D, Baugh C, Sawyer SP, Mroczkowski B, Krahl T, Sarvetnick N: Growth factors in the regenerating pancreas of gamma-interferon transgenic mice. *Lab Invest* 74:985–990, 1996
10. Wang RN, Rehfeld JF, Nielsen FC, Kloppel G: Expression of gastrin and transforming growth factor-alpha during duct to islet cell differentiation in the pancreas of duct-ligated adult rats. *Diabetologia* 40:887–893, 1997
11. Fernandes A, King LC, Guz Y, Stein R, Wright CV, Teitelman G: Differentiation of new insulin-producing cells is induced by injury in adult pancreatic islets. *Endocrinology* 138:1750–1762, 1997
12. Bouwens L: Transdifferentiation versus stem cell hypothesis for the regeneration of islet beta-cells in the pancreas. *Microsc Res Tech* 43:332–336, 1998
13. Bernard C, Berthault MF, Saulnier C, Ktorza A: Neogenesis vs. apoptosis as main components of pancreatic beta cell ass changes in glucose-infused normal and mildly diabetic adult rats. *Faseb J* 13:1195–1205, 1999
14. Mashima H, Ohnishi H, Wakabayashi K, Mine T, Miyagawa J, Hanafusa T, Seno M, Yamada H, Kojima I: Betacellulin and activin A coordinately convert amylase-secreting pancreatic AR42J cells into insulin-secreting cells. *J Clin Invest* 97:1647–1654, 1996
15. Finegood DT, Tzur D, Fieldus WE, McArthur MD, Dhatt D, Dunichand-Hoedel A: β-cell mass dynamics during glucose infusion. *Diabetologia* 40 (Suppl. 1):A120, 1997
16. Githens SD, Holmquist DR, Whelan JF, Ruby JR: Characterization of ducts isolated from the pancreas of the rat. *J Cell Biol* 85:122–135, 1980
17. Bonner-Weir S, Deery D, Leahy JL, Weir GC: Compensatory growth of pancreatic beta-cells in adult rats after short-term glucose infusion. *Diabetes* 38:49–53, 1989
18. Bouwens L, Pipeleers DG: Extra-insular beta cells associated with ductules are frequent in adult human pancreas. *Diabetologia* 41:629–633, 1998
19. Miralles F, Battelino T, Czernichow P, Scharfmann R: TGF-beta plays a key role in morphogenesis of the pancreatic islets of Langerhans by controlling the activity of the matrix metalloproteinase MMP-2. *J Cell Biol* 143:827–836, 1998
20. Wang RN, Bouwens L, Kloppel G: Beta-cell growth in adolescent and adult rats treated with streptozotocin during the neonatal period. *Diabetologia* 39:548–557, 1996
21. Scaglia L, Cahill CJ, Finegood DT, Bonner-Weir S: Apoptosis participates in the remodeling of the endocrine pancreas in the neonatal rat. *Endocrinology* 138:1736–1741, 1997
22. Dahl U, Sjodin A, Semb H: Cadherins regulate aggregation of pancreatic beta-cells in vivo. *Development* 122:2895–2902, 1996
23. Deltour L, Leduque P, Paldi A, Ripoche MA, Dubois P, Jami J: Polyclonal origin of pancreatic islets in aggregation mouse chimeras. *Development* 112:1115–1121, 1991
24. Emmrich J, Weber I, Nausch M, Sparmann G, Koch K, Seyfarth M, Lohr M, Liebe S: Immunohistochemical characterization of the pancreatic cellular infiltrate in normal pancreas, chronic pancreatitis and pancreatic carcinoma. *Digestion* 59:192–198, 1998
25. Friess H, Buchler MW, Mueller C, Malfertheiner P: Immunopathogenesis of chronic pancreatitis (Editorial). *Gastroenterology* 115:1018–1022, 1998
26. Raeder M, Mathisen O: Effect of intravenous infusion of hypertonic glucose solutions on pancreatic HCO3(-) secretion. *Acta Physiol Scand* 115:349–354, 1982